

neutron-production cross sections peak in this energy range. A buncher/chopper beamline has been designed by National Electrostatics Corporation that will produce sub-5-ns pulses at a 4-MHz repetition rate. The target room for the VanDeGraff was designed for neutron production experiments and has the necessary size and shielding for unambiguous calibration of all our planned detectors. The 25-mile distance to the Geneseo campus and ready availability of operating time on the accelerator is a great advantage in rapid turnaround of calibration data.

In summary, we have taken steps to ensure that the neutron diagnostics for the OMEGA Upgrade will meet the needs of the laser-fusion program at LLE. Dedicated target-chamber ports and a neutron flight path will allow control over the scattered-neutron environment in the remote diagnostic room. Diagnostics that require the higher neutron yields expected from the Upgrade, such as the single-hit detector array to measure secondary neutron energy spectra, are now being designed. Diagnostics currently on OMEGA are being redesigned for the Upgrade target chamber and for remote operation in the case of dangerous levels of radioactivity in the target bay. Finally, the availability of a reliable calibration facility at SUNY Geneseo is a great asset in the careful characterization of all the neutron detectors.

#### ACKNOWLEDGMENT

This work was supported by the U.S. Department of Energy Office of Inertial Confinement Fusion under Cooperative Agreement No. DE-FC03-92SF19460 and the University of Rochester. The support of DOE does not constitute an endorsement by DOE of the views expressed in this article.

#### REFERENCES

1. LLE Review **39**, 114 (1989).
2. T. E. Blue and D. B. Harris, Nucl. Sci. Eng. **77**, 463 (1981).
3. LLE Review **27**, 103 (1986); LLE Review **36**, 150 (1988).
4. M. D. Cable and S. P. Hatchett, J. Appl. Phys. **62**, 2233 (1987).
5. R. L. Kremens and M. A. Russotto, presented at the 33rd Annual Meeting of the American Physical Society, Plasma Physics Division, Tampa, FL, 4–8 November 1991.
6. S. M. Lane, E. M. Campbell, and C. Bennett, J. Appl. Phys. **56**, 2027 (1984).
7. H. Azechi *et al.*, Appl. Phys. Lett. **49**, 555 (1986).

## 1.E Temporal Pulse-Width Control of the OMEGA and GDL Laser Oscillators

Flexibility in shaping the temporal profile of the optical pulses applied to laser-fusion targets is a goal for the OMEGA Upgrade. There are several schemes proposed to provide this flexibility.<sup>1–3</sup> The scheme implemented on OMEGA and currently being implemented on GDL involves producing an optical pulse with a laser oscillator and then modifying the temporal profile of this pulse outside the laser oscillator. The final temporal profile depends critically on the

input temporal profile to the pulse-shaping apparatus; that is, it depends on the temporal profile of the pulse out of the laser oscillator. The temporal profile of a pulsed laser depends on the detailed parameters of the laser cavity and intracavity components. Pulse-width control of the current laser oscillators is accomplished through the use of intracavity Fabry-Perot etalons.<sup>2</sup>

On the current OMEGA laser system a short pulse of approximately 70-ps FWHM is produced in a continuous-wave (cw), mode-locked laser and injected into a regenerative amplifier (regen). In the regen the pulse width is stretched with an intracavity Fabry-Perot etalon and amplified to the millijoule level. The output of the regen is then given a steep rising edge by triggering a fast Pockels cell, which removes energy from the beginning of the pulse.<sup>3</sup> In GDL, two regens will be used to produce the main and foot pulses. The two regens will be seeded from the same cw mode-locked laser to maintain synchronization of their output pulses. The two regens differ mainly in the width of their output pulses. The individual pulse widths of the main- and foot-pulse regens will again be controlled by intracavity Fabry-Perot etalons. Until now, little success has been had in analyzing the temporal-mode structure of a laser incorporating one or several etalons.

### **The Fabry-Perot Etalon**

An interferometer consisting of two plane-parallel reflecting surfaces constitutes a Fabry-Perot etalon. The steady-state operation of a Fabry-Perot etalon is well known.<sup>4</sup> For cw input the series of partial waves emitted from an etalon can be summed in closed form to obtain the Airy formula. Concepts such as the free spectral range and the finesse of the etalon are then well defined and can be derived from the Airy formula. When using short pulses or pulses with temporal or phase modulation, a transient analysis is necessary. A rigorous treatment of the transient response of an etalon requires the use of linear systems theory.<sup>5</sup>

When a wave is incident on a plane-parallel etalon, a series of partial waves are transmitted as well as reflected from the etalon. When an etalon is inserted into a laser cavity, it is adjusted so that its surface makes a small angle with the beam lasing in the cavity. If one of the laser end mirrors is flat, tilting the etalon will not misalign the laser cavity in principle since the transmitted waves from the etalon exit the etalon parallel to the input wave regardless of the magnitude of the tilt angle (albeit with some slight translation). On the other hand, the reflected partial waves from the etalon are reflected at a small angle (twice the tilt angle) to the incident wave. The reflected waves from the etalon will eventually be blocked by a limiting aperture in the laser cavity and will be prevented from lasing. For this reason, in the following analysis we only need to consider the transmitted waves through the etalon. The analysis, however, can easily be modified to include a resonant reflector where the reflected waves from the etalon contribute to the laser oscillation.

By the superposition principle for electric fields, the partial waves that exit from an etalon must be added coherently to determine the total output field. This is a linear process, and hence, an etalon comprises a linear system that can be

analyzed using the formalism of linear systems theory.<sup>5</sup> To determine the output of a linear system we need to calculate the impulse-response function of the system. The impulse-response function of an etalon can be determined by calculating the output of the etalon for a delta function input  $\delta(t)$  at time equals zero. The impulse-response function of an etalon having thickness  $d$ , surface-amplitude transmissions  $\gamma_1$  and  $\gamma_2$ , and surface-amplitude reflectivities  $r_1$  and  $r_2$  is given by<sup>6</sup>

$$h(t) = \Gamma \sum_{m=0}^{\infty} R^m \exp(i2mkc\tau) \delta(t - 2m\tau), \quad (1)$$

where  $\tau = dn \cos\theta/c$  is the transit time through the etalon,  $c$  is the speed of light in vacuum,  $n$  is the refractive index of the etalon substrate,  $k$  is the wave number (if the radiation has some finite spread in time then  $k$  is interpreted as the wave number at the central wavelength of the associated bandwidth),  $\theta$  is the angle between the normal to the etalon surface and the incident beam, and  $R = r_1 r_2$  and  $\Gamma = \gamma_1 \gamma_2$  with  $\Gamma = 1 - R$ . The output of the system is given by the convolution

$$E_{\text{out}}(t) = h(t) * E_{\text{in}}(t) = \int_{-\infty}^{\infty} h(\alpha) E_{\text{in}}(t - \alpha) d\alpha \quad (2)$$

of the input field  $E_{\text{in}}(t)$  with the impulse-response function. Performing this operation gives

$$E_{\text{out}}(t) = \Gamma \sum_{m=0}^{\infty} R^m \exp(i2mkc\tau) E_{\text{in}}(t - 2m\tau) \quad (3)$$

for the temporal profile of the output optical field. This equation represents the operation of an etalon on an input optical field to produce an output optical field.

For the special case when  $E_{\text{in}}$  is constant, that is for cw input, the summation in Eq. (3) can be performed in closed form and the result leads to the Airy formula. The physical interpretation of Eq. (3) is straightforward in terms of the coherent summation of partial waves and is given in the literature.<sup>4</sup>

For the more general case when the input to the etalon is an optical pulse, that is  $E_{\text{in}}(t)$  has some temporal profile, the output temporal profile from the etalon again consists of an infinite coherent summation of partial waves. As seen in Eq. (3), each partial wave consists of the input field, translated in time by the etalon round-trip transit time, with amplitude progressively reduced by the reflectivity of the etalon surfaces. For a pulse whose width is of the order of the etalon transit time, severe pulse distortion will occur in the output from the etalon. Figure 53.24 shows the calculated output-intensity temporal profile from an etalon with an input Gaussian-intensity temporal profile having a FWHM pulse width equal to the etalon single-pass transit time. The etalon in this case has surface-intensity reflectivities of 80%, and it is assumed that all partial waves add in phase so that the phase term in Eqs. (1) and (3) is unity. In general, the output

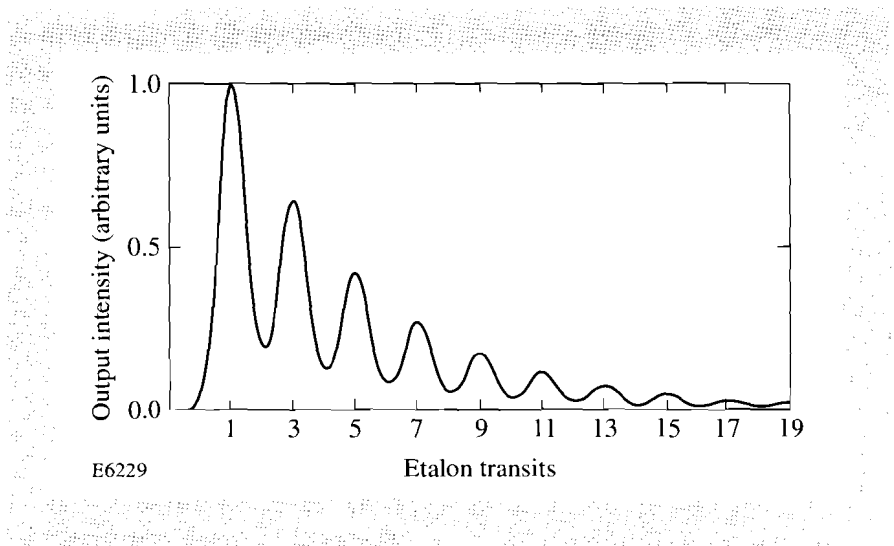


Fig. 53.24

The output-intensity profile from an etalon with an input Gaussian-intensity profile having a FWHM pulse width equal to the etalon single-pass transit time.

of an etalon is stretched in time with a right-left asymmetry in the pulse shape and with some degree of temporal modulation, as illustrated in Fig. 53.24. The temporal modulation and the right-left asymmetry have been observed in the output of a regenerative amplifier and are discussed in the experimental section.

In a regenerative amplifier with an intracavity etalon, a short pulse (short compared to the laser-cavity round-trip time) is injected into the laser cavity and makes many round trips in the cavity. This pulse is amplified and operated on by the etalon during each pass in the laser cavity. The temporal profile of the pulse in the cavity can be calculated after each pass from Eq. (3) given the input temporal profile to the etalon. The output profile from the etalon after each pass becomes the input profile to the etalon for the next pass. Knowing the injected pulse temporal profile, the process can be iterated for each laser-cavity round trip to determine the final output temporal profile of the regenerative amplifier. If the final pulse width emitted by the regenerative amplifier is comparable to the regenerative-amplifier cavity round-trip transit time, then the effects of the regenerative-amplifier cavity on the pulse width must be taken into account.

### **Etalons Inside a Laser Cavity**

An intracavity etalon can be used to increase the pulse width emitted by a regenerative amplifier. If the temporal pulse width of the radiation in the regenerative-amplifier laser cavity becomes of the order of the laser-cavity round-trip time, then the effect of the laser cavity itself must be taken into consideration. This can be accomplished by calculating the impulse-response function for a single pass or for a round trip through the laser cavity including the etalons, and then iterating this for each pass or laser-cavity round trip as previously described.

To calculate the impulse-response function for a round trip in the laser cavity we begin by tracing a delta-function input around the laser cavity in a round trip. We decompose the laser-cavity round-trip operation into space propagation and the operation of the etalons. The laser-cavity round-trip propagation is shown

schematically in Fig. 53.25 as five separate operations. The operations with their impulse-response functions are  $h_{L1}(t)$  for propagation from the end mirror to the etalon and through the etalon for propagation over an optical distance  $L1$ ,  $h_e(t)$  for the operation of the etalon,  $h_{L2}(t)$  for propagation from the etalon to the end mirror and back to the etalon and through the etalon for propagation over an optical distance  $L2$ ,  $h_e(t)$  for the second operation of the etalon, and  $h_{L3}(t)$  for propagation back to the first mirror over a distance  $L3$ . If we cascade the previously mentioned operations (the convolutions can be performed in any order) we obtain the impulse-response function corresponding to a round trip in the laser cavity given by

$$h_s(t) = h_{L1}(t) * h_{L2}(t) * h_{L3}(t) * h_e(t) * h_e(t). \quad (4)$$

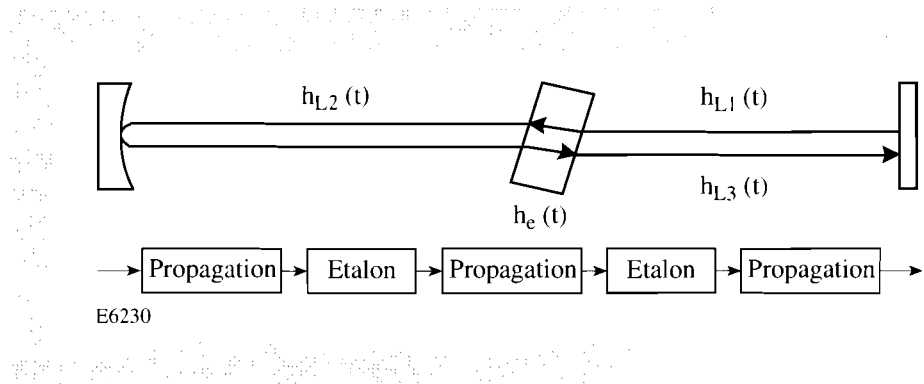


Fig. 53.25  
The impulse-response function corresponding to a round trip in a laser cavity with an intracavity etalon represented as a cascade of five operations in the laser cavity.

The impulse-response function corresponding to propagation over the optical distance  $L$  is given by

$$h_L(t) = \alpha \delta(t - \tau_L) \exp(ikL), \quad (5)$$

where  $\tau_L$  is the propagation time over the optical distance  $L$ , and  $\alpha$  represents the linear amplitude gain or loss in the propagation. Equation (4) with Eq. (5) for the individual space propagations and Eq. (1) for the operation of the etalon gives

$$h_s(t) = \Gamma_c \Gamma^2 \exp(ikL) \sum_{\ell=0}^{\infty} \sum_{m=0}^{\infty} R^{(m+\ell)} \exp[i2kc\tau(m+\ell)] \delta[t - \tau_c - 2\tau(m+\ell)] \quad (6)$$

for the system impulse-response function, where  $\Gamma_c = r_{1c} r_{2c} \gamma_{1c}$  is the product of the laser-cavity end-mirror amplitude reflectivities  $r_{1c}$   $r_{2c}$  and amplitude transmission  $\gamma_{1c}$  of the laser-output coupler,  $L = L1 + L2 + L3$  is the total round-trip optical distance in the laser cavity (including etalons),  $\tau_c = \tau_1 + \tau_2 + \tau_3$  is the laser-cavity round-trip time, and the remainder of the variables are defined as in Eq. (3). The output of the system after one laser-cavity round trip is then given by

$$E_{out}(t) = \Gamma_c \Gamma^2 \exp(ikL) \sum_{\ell=0}^{\infty} \sum_{m=0}^{\infty} R^{(m+\ell)} \exp[i2kc\tau(m+\ell)] E_{in}[t - \tau_c - 2\tau(m+\ell)] \quad (7)$$

in terms of the input to the system and the appropriate variables as defined previously. Often times it is necessary to insert two etalons in the laser cavity. With a straightforward extension of the preceding procedure we obtain the expression

$$E_{\text{out}}(t) = \Gamma_c \Gamma_{e1}^2 \Gamma_{e2}^2 \exp(ikL) \sum_{\ell_2=0}^{\infty} \sum_{m_2=0}^{\infty} \sum_{\ell_1=0}^{\infty} \sum_{m_1=0}^{\infty} R_{e1}^{m_1+\ell_1} R_{e2}^{m_2+\ell_2} \exp[i2kc\tau_{e1}(m_1+\ell_1)] \exp[i2kc\tau_{e2}(m_2+\ell_2)] E_{\text{in}}[t-\tau_c-2\tau_{e1}(m_1+\ell_1)-2\tau_{e2}(m_2+\ell_2)] \quad (8)$$

for the output of a regenerative amplifier with two etalons. [Equation (8) assumes a “cold cavity” with no gain. When operating in the small-signal gain region of the laser and for an injected pulse having a narrow bandwidth compared to the gain bandwidth, the gain will only affect the amplitude of the output pulse and not the temporal profile. This is a good approximation for the experiments described in the experimental section.] In Eq. (8) there are two summations for each etalon since the etalons are double passed in one laser-cavity round trip. Further generalizations to a laser cavity with several etalons are straightforward. Note that the no-etalon case corresponds to the  $\ell_1, m_1, \ell_2,$  and  $m_2 = 0$  term in Eq. (8). This term reduces to Eq. (5) and corresponds to propagation over the round-trip distance  $L$  in the laser cavity, where  $L$  becomes twice the laser-cavity length and  $\tau_c$  becomes the laser-cavity round-trip time with  $kL$  the accumulated phase on a round trip. For the case when the final pulse width is of the order of the laser-cavity round-trip time or larger, the oscillator condition requires that the phase shift on a round trip through the laser cavity be an integer multiple of  $2\pi$  (i.e.,  $kL = p2\pi$  for  $p$  an integer). For optimum injection in this case, we require that the laser-cavity length be an integer multiple of the center wavelength of the injected pulse into the regenerative amplifier and that the etalon be tuned for maximum transmission at this wavelength.

### Thermal Sensitivity

To determine the temperature sensitivity of a regenerative amplifier with an intracavity etalon we examine the thermal-mechanical properties of the etalon. When a regenerative amplifier is aligned, the etalon is angle tuned such that the partial waves from the etalon all add in phase. If the temperature drifts after the initial alignment, the operation of the etalon changes and an effective loss will be introduced into the regenerative-amplifier laser cavity. Both the index of refraction  $n$  and the etalon thickness  $d_e$  depend on temperature. The exact treatment of the temperature sensitivity of a regenerative amplifier with an intracavity etalon is complex. To approximate the temperature sensitivity of an etalon we examine the change in the output field [given by Eq. (3)] for a small change in temperature. If we allow the output field represented by Eq. (3) to depend on temperature and expand the optical path length in the etalon about  $\Delta T$  (keeping only the lowest-order terms), then the field at a slightly different temperature  $T + \Delta T$  can be approximated by

$$E_{\text{out}}(t, T + \Delta T) = \Gamma \sum_{m=0}^{\infty} R^m \exp\left\{i2mk \left[ nd_e + \frac{d(nd_e)}{dT} \Delta T \right]\right\} E_{\text{in}}(t - 2m\tau) . \quad (9)$$

Here we have only considered the change in the phase relationship of the partial waves exiting the etalon and have neglected the change in transit time  $\tau$  in the last factor of Eq. (3). This small change in temperature causes the small change  $\left[ d(nd_e)/dT \right] \Delta T$  in the single-pass optical path length through the etalon. If the single-pass optical path length through the etalon changes by one-half wavelength, then the etalon will tune through one free spectral range. The temperature change required to change the bandpass of the etalon by one free spectral range is then given by

$$\Delta T = \frac{\lambda/2}{\left[ \frac{d(nd_e)}{dT} \right]} = \frac{\lambda/2}{\left[ n \frac{d(d_e)}{dT} + d_e \frac{d(n)}{dT} \right]} \quad (10)$$

For a 4-mm fused-silica etalon  $n = 1.45$ ,  $1/d_e d(d_e)/dT = 0.55 \times 10^{-6}/^\circ\text{C}$ ,  $dn/dT = 10.3 \times 10^{-6}/^\circ\text{C}$ ,<sup>7</sup> and for  $\lambda = 1053$  nm we get  $\Delta T = 11.9^\circ\text{C}$  to tune the etalon through one free spectral range. This value has been verified experimentally and is discussed in the next section.

### Experiment

Verification of the preceding theory has been performed through a series of experiments with intracavity etalons. A set of fused-silica etalons having 50% reflecting surfaces and varying thicknesses were tested in a regenerative amplifier. The surfaces of the etalons were coated in two coating runs (one per surface) to ensure uniformity of the reflective coatings among the etalons. The etalons were temperature controlled to within  $0.1^\circ\text{C}$  in order to stabilize their properties. An Nd:YLF regenerative amplifier was seeded with a 70-ps-FWHM pulse from a cw mode-locked Nd:YLF laser. Pulses from the cw mode-locked laser were injected into the regenerative amplifier by polarization coupling off the regenerative-amplifier intracavity polarizer. At the peak of the gain profile of the flash-lamp-pumped Nd:YLF rod, a pulse was locked into the laser cavity by rapidly changing the state of the laser-cavity Q-switch in less than the laser-cavity round-trip time. Once locked in the laser cavity, the injected pulse experienced gain and was operated on by the intracavity etalons during each successive round trip in the laser cavity. The 50% reflecting end mirror of the regenerative amplifier was used as an output coupler. The injected pulse made several round trips in the laser cavity, after which a Q-switched, mode-locked-type pulse train was emitted with pulses in the pulse train separated by the laser-cavity round-trip time of 13 ns. The buildup time of the laser cavity (i.e., the time between when the pulse is locked into the laser cavity until the pulse is emitted by the laser cavity) was measured to determine the number of round trips that the injected pulse made in the laser cavity.

The buildup time of the regenerative amplifier could be changed by varying the gain in the laser rod. Decreasing the gain causes the buildup time to increase, and conversely, increasing the gain causes the buildup time to decrease. Figure

53.26 shows the FWHM output pulse width of the regenerative amplifier versus the number of round trips that the injected pulse makes in the laser cavity for a 4-mm etalon. Also shown in this figure is the left-half width at half maximum (left HWHM) and right-half width at half maximum (right HWHM) for each data point. The left HWHM is the half width of the beginning of the pulse and the right HWHM is the half width of the end of the pulse. The solid curves in the figure correspond to the previously mentioned theory with the upper curve corresponding to the FWHM of the pulse, the center curve corresponding to the right HWHM of the pulse, and the lower curve corresponding to the left HWHM of the pulse. Note that after just one round trip in the laser cavity the pulse develops a left-right asymmetry in the pulse temporal profile indicating a sharper rising edge than falling edge. This is as expected from the discussion on the operation of a single etalon. This asymmetry persists but does not change significantly as the number of round trips in the laser cavity increases.

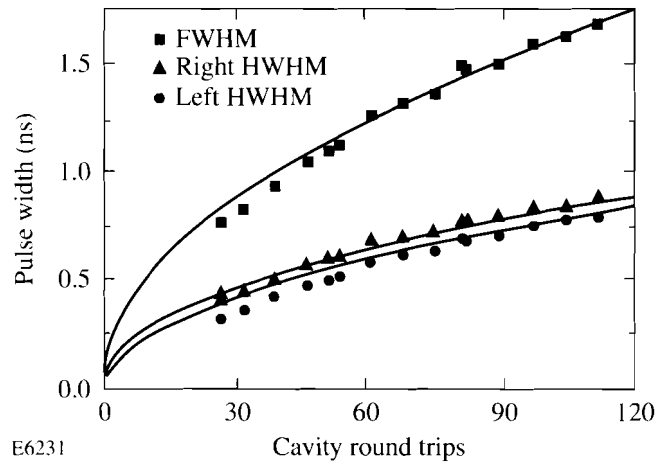


Fig. 53.26

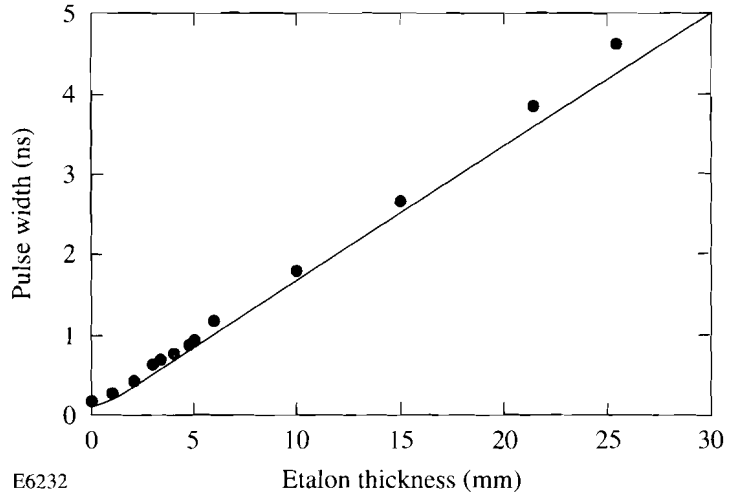
The output pulse width of a regenerative amplifier with 4-mm intracavity etalon plotted versus the number of round trips the injected pulse makes in the laser cavity. The solid curves correspond to a calculation of the pulse FWHM (upper curve), right HWHM (middle curve), and left HWHM (lower curve). The left- and right-half widths show the asymmetry in the pulse profile.

Figure 53.27 shows the output pulse width of the regenerative amplifier versus the etalon thickness for the set of etalons. All measurements in Fig. 53.27 were taken with the same buildup time corresponding to 27 laser-cavity round trips for the injected pulse. The solid curve in the figure corresponds to the previously mentioned theory with the appropriate experimental conditions.

For a single, thick intracavity etalon (i.e., the injected pulse width is shorter than the etalon transit time) severe temporal modulation is observed. Figure 53.28 shows the output of the regenerative amplifier for the 25.4-mm etalon taken with a 4.5-GHz SCD5000 Tektronix digitizing oscilloscope and a fast vacuum photodiode (response time approximately 100 ps). The injected pulse made approximately 60 round trips in the laser cavity. For this case, the 70-ps, FWHM-injected pulse is shorter than the 123-ps etalon transit time. As seen in Fig. 53.28, the output of the regenerative amplifier has the temporal modulation expected from an iteration of Eq. (3) and as depicted in Fig. 53.24 for a similar case. Figure 53.29 shows a calculation of the pulse temporal profile for this case

Fig. 53.27

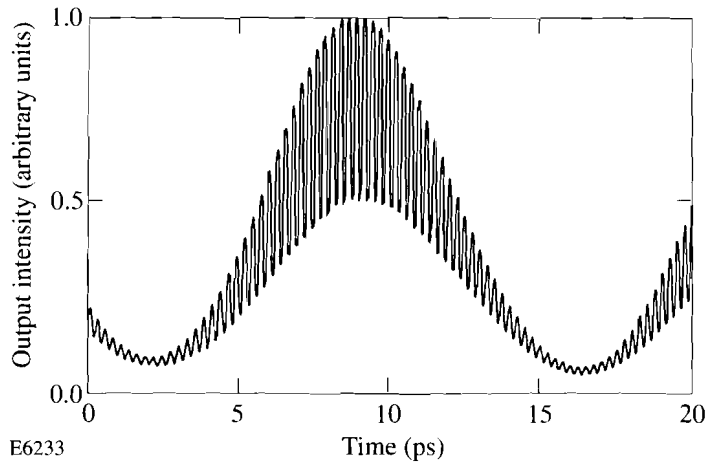
The output pulse width (FWHM) of a regenerative amplifier with intracavity etalon plotted versus the etalon thickness. The injected 70-ps pulse (FWHM) made 27 round trips in the regenerative-amplifier cavity. All etalons were fused silica with 50% reflective coatings on both surfaces.



E6232

Fig. 53.28

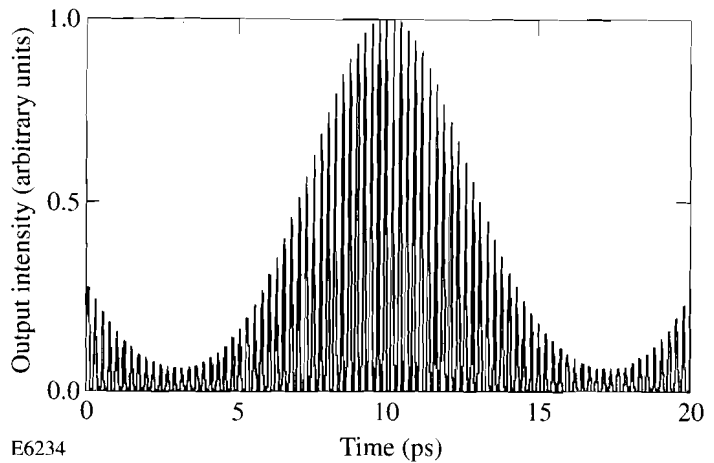
The measured output-intensity temporal profile of a regenerative amplifier with a 25.4-mm intracavity etalon. The response time of the detection system was approximately 100 ps.



E6233

Fig. 53.29

The calculated output-intensity temporal profile of a regenerative amplifier with a 25.4-mm intracavity etalon. The calculation used a 2-ps time resolution.



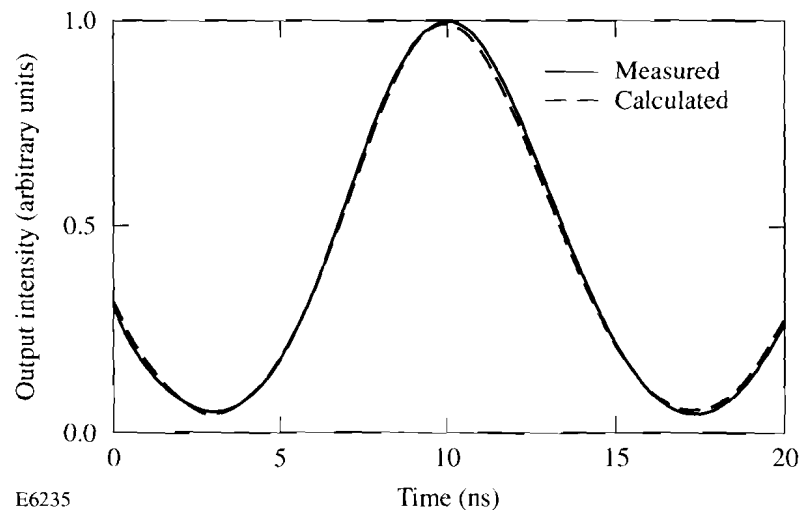
E6234

based on the previously mentioned theory assuming that the etalon is tuned with all partial waves in phase and that the oscillator cavity condition is satisfied. The calculation was made with a 2-ps time resolution. The depth of modulation of the data in Fig. 53.28 is limited by the bandwidth of the measurement equipment.

To eliminate the temporal modulation shown in Fig. 53.28 a second intracavity etalon was used. Insertion of a 5-mm etalon in addition to the 25.4-mm etalon produced the output shown in Fig. 53.30 for the same experimental conditions. The envelope of the pulse in Fig. 53.30 shows the injected 70-ps-FWHM pulse stretched to 7-ns FWHM. Here the 7-ns pulse width is comparable to the 13-ns, laser-cavity round-trip time, and some pulse overlap effects can be seen between pulses in the pulse train. The corresponding theoretical calculation can also be seen in Fig. 53.30. For the calculation, 70 cavity round trips were assumed, which corresponded well with the measured cavity buildup time. Also used in the calculation was a  $1.2\pi$  phase shift per round trip in the cavity. (The laser-cavity length was not controlled, and hence, a constant phase shift with arbitrary value between 0 and  $2\pi$  occurred every cavity round trip. The assumed  $1.2\pi$  phase shift per cavity round trip gave the best fit to the data.) Closer examination of the output pulse showed the temporal profile to be modulation free, both theoretically with 4-ps resolution and experimentally with the  $\sim 100$ -ps resolution limited by the bandwidth of the measurement equipment. We would expect no measurable modulation on even faster time scales; however, streak-camera measurements with higher temporal resolution are planned. The 7-ns pulse width was not limited and could, in principle, be stretched to any desired value.

Fig. 53.30

The measured and calculated output-intensity temporal profiles of a regenerative amplifier with a 25.4-mm and a 5-mm intracavity etalon. The response time of the detection system was approximately 100 ps. The calculation used a 4-ps time resolution.



To produce repeatable laser output, the intracavity etalons were temperature stabilized and angle tuned to minimize the buildup time for the output pulse envelope. This corresponds to all partial waves of the etalons adding in phase to maximize the transmission of the etalon and minimize the intracavity losses. If

the etalon is not tuned in angle and temperature, the transmission of the etalon will be less than 100%. In that case, some of the power incident on the etalon will be reflected at an angle to the cavity lasing mode and blocked by an intracavity aperture. This would represent a loss to the laser cavity that would manifest itself as an increase in the laser buildup time. To test the temperature sensitivity of an intracavity etalon, the temperature of a 4-mm etalon was increased after it was angle tuned in the laser cavity. As the etalon temperature increased, the buildup time of the laser cavity increased to a certain value. As the temperature continued to increase, the buildup time began to decrease. After a temperature increase of approximately 12°C, the buildup time returned to its original value indicating that the etalon was tuned through one free spectral range. By decreasing the temperature to its original value, the process repeated itself in reverse and the buildup time again returned to its original value. This result agrees well with the calculated thermal sensitivity previously mentioned.

### Implementation

Regenerative amplifiers have been installed in OMEGA with pulse-shaping capability.<sup>3</sup> A 70-ps-FWHM pulse from a cw mode-locked laser is injected into a regenerative amplifier. The system regen operates with a 4-mm-thick etalon with 50% reflective coatings on each surface. After the injected pulse makes approximately 40 round trips in the cavity, a 650-ps pulse is emitted. The etalon is housed in a copper block and is temperature controlled to 0.1°C. When pulses having a sharp rising edge are required, a 5-mm-thick etalon is inserted into the cavity producing approximately 1.3-ns pulses for the same conditions. These longer pulses are then shaped with a photoconductively switched Pockels cell.

The design of the GDL regens are similar to the OMEGA regens. In GDL the main-pulse laser will use an intracavity etalon with approximately 4-mm thickness. The timing scheme for GDL is simplified such that pulse-width control will be achieved by simply changing the buildup time (gain) of the regen, followed by moving the output pulse in time so as to be synchronous with the rest of GDL timing. This choice of etalon should allow a range of 500- to 1000-ps output pulse width. The foot-pulse regen will use two etalons having thicknesses of 5 mm and 25 mm, respectively. This combination of etalons should allow for temporally smooth pulses with approximately 5- to 6-ns pulse width. All etalons will be temperature controlled to within 0.1°C.

### Summary

A regenerative amplifier with intracavity etalons has been analyzed and tested. The analysis is based on linear systems theory. The analysis can predict the output temporal profile of a regenerative amplifier given the input injected-pulse temporal profile and the details of the laser-cavity and intracavity etalons. The output temporal profile of the regenerative amplifier was measured as we varied the etalon thickness and the number of round trips that the injected pulse made in the laser cavity. Temporal modulation on the output pulse was calculated and observed for a single thick intracavity etalon. An injected pulse 70-ps wide was stretched to 7 ns with no temporal modulation using two etalons. The effect of raising the temperature of an etalon was also measured and analyzed. A 12°C change in the etalon temperature tuned the etalon through one free